

# SEARCH FOR NEW SOLID STATE LITHIUM-ION CONDUCTORS

Hiroyuki Oguchi<sup>1,2\*</sup>, M. Matsuo<sup>2</sup>, S. Orimo<sup>2</sup>, H. Kuwano<sup>1</sup>

<sup>1</sup>Department of Nano-Mechanics, Graduate School of Engineering, Tohoku University, Sendai, Japan

<sup>2</sup>Institute for Materials Research, Tohoku University, Sendai, Japan

Presenting Author: h.oguchi@imr.tohoku.ac.jp

**Abstract:** We have experimentally searched new solid state lithium-ion conductors for thin film lithium-ion batteries using ac complex impedance measurements, and found superior lithium-ion conductivity in two materials  $\text{LiBH}_4$  and  $\text{Li}_3\text{AlH}_6$ . The conductivities of  $\text{LiBH}_4$  and  $\text{Li}_3\text{AlH}_6$  at room temperature (RT) were  $4.1 \times 10^{-8}$  S/cm and  $1.4 \times 10^{-7}$  S/cm, respectively.  $\text{LiBH}_4$  exhibited lithium fast-ionic conductivity of higher than  $1.0 \times 10^{-3}$  S/cm accompanied by a structural transition. We also demonstrated the enhancement of the conductivity of these materials by addition of lithium iodide LiI. By adding 0.33 molar ratio of LiI into  $\text{LiBH}_4$  and  $\text{Li}_3\text{AlH}_6$ , the conductivity at RT increased about 1000 times for the former and about 35 times for the latter.

**Keywords:** MEMS, micro power supply, thin film lithium-ion battery, complex hydride, solid state electrolyte

## INTRODUCTION

Thin film lithium-ion batteries [1-4] enabling batteries' integration with other micro devices onto a single chip may be an appropriate choice for micro power supplies of microelectromechanical systems (MEMS). One good example may be micro sensor nodes, where thin film lithium-ion batteries, micro sensors, and micro energy harvesters [5-8] are integrated. This kind of sensor nodes do not ask us to replace batteries periodically because micro sensors will consume energy stored in thin film lithium-ion batteries which are replenished by micro energy harvesters obtaining energy from the environment in the form of vibration et al. Such micro sensor nodes with less maintenance are essential to establish sensor communication society [9], where a large number of micro sensor nodes are distributed from place to place.

In order to establish reliable thin film lithium-ion batteries, one of the keys is to develop solid state electrolytes with high lithium-ion conductivity along with electrical and chemical stability. Thus, so far, many researchers have been working on the search for solid state electrolytes, and developed various classes of materials such as oxides [10, 11], sulfides [12, 13], nitrides [14], and halides [15, 16]. However, there is no material satisfying all requirements at once. Thus further materials' search is necessary in another class of materials whose lithium-ion conductivity have not been investigated. For this purpose, we searched  $\text{LiBH}_4$  and  $\text{Li}_3\text{AlH}_6$ , those are complex hydrides with ionic bonding between  $\text{Li}^+$  cation and  $(\text{BH}_4)^-$  or  $(\text{AlH}_6)^{3-}$  complex anions.

$\text{LiBH}_4$  and  $\text{Li}_3\text{AlH}_6$  are electrical insulators with a wide bandgap [17-19]. The crystal structures at RT are different between these complex hydrides, that is, orthorhombic phase for  $\text{LiBH}_4$  [20] and trigonal phase for  $\text{Li}_3\text{AlH}_6$  [21]. In addition,  $\text{LiBH}_4$  shows structural phase transition between low temperature (LT, orthorhombic) phase and high temperature (HT, hexagonal) phase at around 390 K (Fig. 1). The coordination number of  $\text{Li}^+$  cation [21, 22], ionic

radius [23] and valence of anions of these hydrides (listed in Table I) are also different between these complex hydrides.

In this paper, we report on the investigation of lithium-ion conductivity in  $\text{LiBH}_4$  and  $\text{Li}_3\text{AlH}_6$ . We also discuss the enhancement of the conductivity of these complex hydrides by addition of lithium iodide LiI.

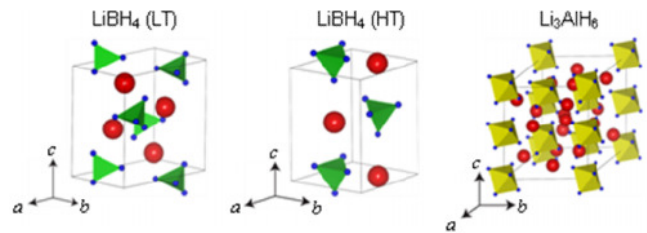


**FIG. 1.** The schematic crystal structure of LT phase and HT phase of  $\text{LiBH}_4$ , and  $\text{Li}_3\text{AlH}_6$ . Large and small circles correspond to Li and H atoms, respectively. B atoms are embedded in  $(\text{BH}_4)^-$  tetrahedra. Al atoms are embedded in  $(\text{AlH}_6)^{3-}$  octahedra.

**Table I.** Coordination number of  $\text{Li}^+$  cation, and complex anion's ionic radius and valence of LT phase of  $\text{LiBH}_4$ , HT phases of  $\text{LiBH}_4$ , and  $\text{Li}_3\text{AlH}_6$ .

	Coordination number of $\text{Li}^+$ cation	Complex anion	
		Ionic radius (nm)	Valence [formula]
LT phase of $\text{LiBH}_4$	9 <sup>b</sup>	0.205 <sup>d</sup>	1
HT phase of $\text{LiBH}_4$	13 <sup>b</sup>		$[(\text{BH}_4)]$
$\text{Li}_3\text{AlH}_6$	6 <sup>c</sup>	0.256 <sup>d</sup>	3 $[(\text{AlH}_6)^{3-}]$

<sup>b</sup>Reference 20

<sup>c</sup>Reference 21

<sup>d</sup>Reference 23

## EXPERIMENTAL

LiBH<sub>4</sub> was purchased from Aldrich Co. Ltd. Li<sub>3</sub>AlH<sub>6</sub> was synthesized by mechanical milling of appropriate amounts of LiH and LiAlH<sub>4</sub> (LiH and LiAlH<sub>4</sub> were purchased from Alfa Aesar and Aldrich Co. Ltd., respectively) for 5 h under a He atmosphere and subsequent heat treatment at 383 K for 20 h. LiI (purchased from Aldrich Co. Ltd.) with nominal compositions of LiBH<sub>4</sub>+xLiI ( $x = 0, 0.07, 0.14, 0.20, 0.33,$  and  $1.00$ ) and Li<sub>3</sub>AlH<sub>6</sub>+xLiI ( $x = 0$  and  $0.33$ ) were mechanically milled. The samples were examined by powder x-ray diffraction (XRD) (Cu K $\alpha$  radiation, RT). The electrical conductivity was determined by ac complex impedance measurements between RT and 393 K or 433 K in heating and cooling runs. A pair of Li or Au foils was used as the electrodes. The samples were always handled in a glove box filled with purified Ar/He.

## RESULTS AND DISCUSSION

Figure 2 shows the temperature dependence of the electrical conductivity of LiBH<sub>4</sub>+xLiI ( $x = 0, 0.33$ ). In heating process, the conductivity of LiBH<sub>4</sub> increased with increasing temperature. A discontinuous jump was observed at around 390 K, which corresponds to the structural transition temperature from the LT phase to the HT phase. The conductivity in the HT phase was as high as 10<sup>-3</sup> S/cm, which is comparable to those of high lithium-ion conductors [11, 24-27] at room temperature. Below and above 390 K, the temperature dependences of the conductivity showed Arrhenius behaviors. The activation energies  $E_a$  for the conduction were evaluated using the equation

$$\sigma T = \sigma_0 \exp(-E_a/k_B T)$$

where  $\sigma$  is the conductivity,  $\sigma_0$  is the preexponential parameter, and  $k_B$  is the Boltzmann constant. We obtained  $E_a$  of 0.69 and 0.53 eV for the LT phase and the HT phase, respectively.

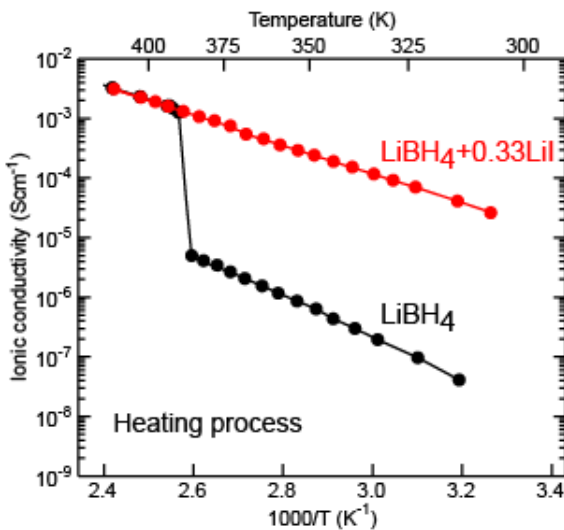


Figure 2. Temperature dependence of the conductivity of LiBH<sub>4</sub> (black) and LiBH<sub>4</sub>+0.33LiI (red).

The effect of addition of LiI on the conductivity of LiBH<sub>4</sub> was evaluated by comparing the conductivity of LiBH<sub>4</sub>+0.33LiI with the conductivity of LiBH<sub>4</sub> (see Fig. 2). In contrast to LiBH<sub>4</sub>, LiBH<sub>4</sub>+0.33LiI showed no apparent transition within the temperature range of this measurement. As a result, the conductivity at RT became approximately 1000 times higher for LiBH<sub>4</sub>+0.33LiI than that for LiBH<sub>4</sub>.

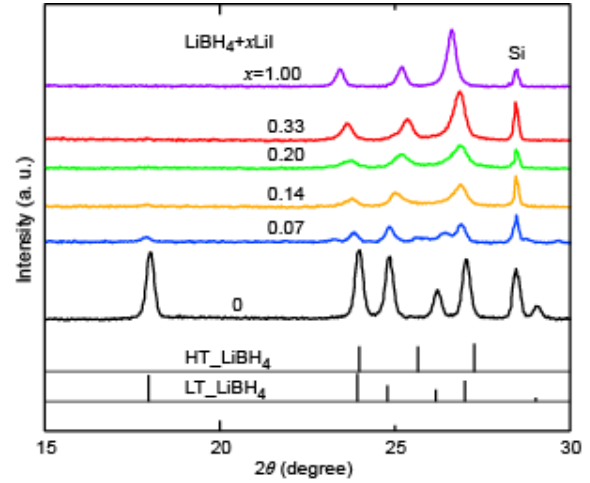


Figure 3. XRD patterns of LiBH<sub>4</sub>+xLiI ( $x = 0, 0.07, 0.14, 0.20, 0.33,$  and  $1.00$ ). Positions of the diffraction peaks are calibrated by Si internal standard.

Table II. Lattice constants,  $a$  and  $c$ , of the HT phase of LiBH<sub>4</sub>+xLiI for  $x = 0, 0.33,$  and  $1.00$ . Lattice constants for  $x = 0.07, 0.14,$  and  $0.20$  are left blank as none of them are indexed by orthorhombic and hexagonal unit cells. Lattice constants of (hexagonal-)LiI are also added for reference.

$x$ in LiBH <sub>4</sub> + xLiI	$a$	$c$
	(Å)	
0	4.24±0.02 <sup>a</sup>	6.87±0.03 <sup>a</sup>
0.07	-	-
0.14	-	-
0.20	-	-
0.33	4.354±0.002	7.035±0.005
1.00	4.389±0.001	7.073±0.003
LiI	4.514±0.001 <sup>b</sup>	7.311±0.002 <sup>b</sup>

<sup>a</sup>Reference 28

<sup>b</sup>Reference 29

The origin responsible for the higher conductivity of LiBH<sub>4</sub> due to addition of LiI was examined by powder XRD at RT. Figure 3 shows the powder XRD patterns of LiBH<sub>4</sub>+xLiI ( $x = 0, 0.07, 0.14, 0.20, 0.33,$  and  $1.00$ ). The diffraction peak intensities of the LT phase of LiBH<sub>4</sub> ( $x = 0$ ) drastically decrease with  $x = 0.07$ . Only the peaks corresponding to the HT phase

can be detected with  $x = 0.33$  and  $1.00$ . This indicated that the higher conductivity of  $\text{LiBH}_4$  is attributed to the stabilization of the HT phase of  $\text{LiBH}_4$  at RT by addition of  $\text{LiI}$ . The  $\text{LiBH}_4 + x\text{LiI}$  pseudobinary system probably forms  $\text{Li}(\text{BH}_4\text{-I})$  solid-solutions, similar to  $\text{Li}(\text{Br-I})$  in the  $\text{LiBr} + x\text{LiI}$  system [30]. The lattice constants of the HT phase ( $x = 0, 0.33$  and  $1.00$ ) summarized in Table II are found to increase with increasing  $x$ ; as is well comparable with the previous estimation of the unit-cell volumes [31].

The conductivities of  $\text{Li}_3\text{AlH}_6 + x\text{LiI}$  ( $x = 0, 0.33$ ) were then investigated, and the results are shown in Fig. 4. Temperature dependences of the conductivity of  $\text{Li}_3\text{AlH}_6$  showed Arrhenius behaviors between RT and 393 K; the conductivity increased almost linearly from  $1.4 \times 10^{-7}$  to  $1.6 \times 10^{-5}$  S/cm for  $\text{Li}_3\text{AlH}_6$ . In addition,  $E_a$  of  $\text{Li}_3\text{AlH}_6$  was 0.61 eV. This value is comparable with  $E_a$  of the LT phase of  $\text{LiBH}_4$ . In contrast to  $\text{LiBH}_4$ ,  $\text{Li}_3\text{AlH}_6$  did not show conductivity jump.

The effect of addition of  $\text{LiI}$  on the conductivity of  $\text{Li}_3\text{AlH}_6$  was evaluated by comparing the conductivity of  $\text{Li}_3\text{AlH}_6 + 0.33\text{LiI}$  with the conductivity of  $\text{Li}_3\text{AlH}_6$  (see Fig. 4). At RT, the conductivity became about 35 times higher for  $\text{Li}_3\text{AlH}_6 + 0.33\text{LiI}$  than that for  $\text{Li}_3\text{AlH}_6$ . The addition of  $\text{LiI}$  also decreased  $E_a$  to 0.48 eV, which is a value smaller than that of the HT phase of  $\text{LiBH}_4$  (0.53 eV).

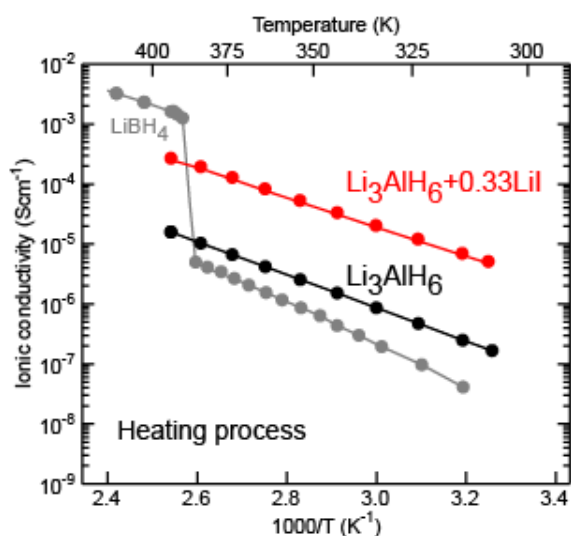


Figure 4. Temperature dependence of the conductivity of  $\text{Li}_3\text{AlH}_6$  (black) and  $\text{Li}_3\text{AlH}_6 + 0.33\text{LiI}$  (red).

The origin responsible for the higher conductivity of  $\text{Li}_3\text{AlH}_6$  due to addition of  $\text{LiI}$  may be the increase of carrier concentration caused by a dispersion of residual  $\text{LiI}$  [32], which is indicated by remaining XRD diffraction peaks of  $\text{LiI}$  (Fig. 5). Decomposition, hydration, and compounds formation were not likely to have been responsible for the enhancement of conductivity, because no XRD diffraction peaks other than those of  $\text{Li}_3\text{AlH}_6$  and  $\text{LiI}$  were observed.

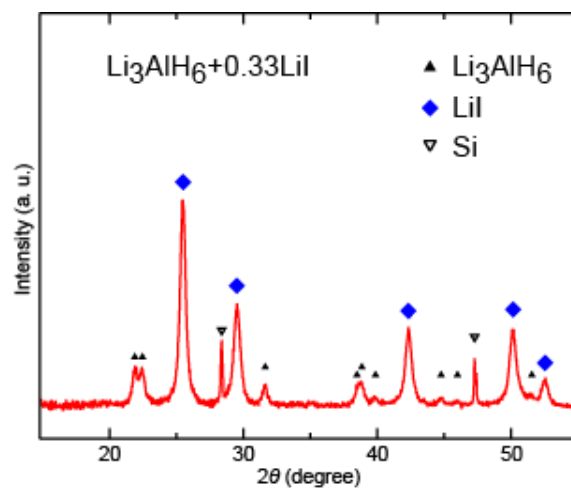


Figure 5. XRD patterns of  $\text{Li}_3\text{AlH}_6 + 0.33\text{LiI}$ . Positions of the diffraction peaks are calibrated by Si internal standard.

## CONCLUSION

We have experimentally investigated the electrical conductivity in  $\text{LiBH}_4$  and  $\text{Li}_3\text{AlH}_6$  using ac complex impedance measurements in order to search new solid state lithium-ion conductors which are applicable as solid state electrolytes of thin film lithium-ion batteries. The conductivity of  $\text{LiBH}_4$  and  $\text{Li}_3\text{AlH}_6$  at RT were  $4.1 \times 10^{-8}$  S/cm and  $1.4 \times 10^{-7}$  S/cm, respectively. The conductivity of  $\text{LiBH}_4$  jumped by three orders of magnitude due to structural transition at approximately 390 K. The HT phase of  $\text{LiBH}_4$  exhibited a high conductivity of the order of  $10^{-3}$  S/cm. By addition of  $\text{LiI}$ , the conductivities at RT were enhanced about 1000 times for  $\text{LiBH}_4$  and about 35 times for  $\text{Li}_3\text{AlH}_6$ . We have succeeded in imparting room-temperature high lithium-ion conductivity to complex hydrides which had not been considered as lithium-ion electrolytes. We believe that discovery of lithium-ion conductivity in  $\text{LiBH}_4$  and  $\text{Li}_3\text{AlH}_6$  have broadened options of the solid state electrolytes of the thin film lithium-ion batteries, which will be integrated into micro devices as micro power sources.

## ACKNOWLEDGEMENT

This work was partially supported by; KAKENHI, the Creative Scientific Research Program (No. 18GS0203: Study of nano-energy system creation), Scientific Research (A) (No. 21246100) and (S) (No. 17106008), and the Global-COE Program “Materials Integration (Tohoku University)”.

## REFERENCES

- [1] Iriyama Y, Yada C, Abe T, Ogumi Z, Kikuchi K 2006 A new kind of all-solid-state thin-film-type lithium-ion battery developed by applying a D.C. high voltage *Electrochem. Commun.* **8** 1287-1291
- [2] Bates J B, Gruzalski G R, Dudney N J, Luck C F, Yu X 1994 Rechargeable thin-film lithium

- batteries *Solid State Ionics* **70/71** 619-628
- [3] Souquet J L, Duclot M 2002 Thin film lithium batteries *Solid State Ionics* **148** 375-379
- [4] Kuwata N, Kawamura J, Toribami K, Hattori T, Sata N 2004 Thin-film lithium-ion battery with amorphous solid electrolyte fabricated by pulsed laser deposition *Electrochem. Commun.* **6** 417-421
- [5] Donelan J M, Naing Q L V, Hoffer J A, Weber D J, Kuo A D 2008 Biomechanical Energy Harvesting: Generating Electricity During Walking with Minimal User Effort *Science* **319** 807-810
- [6] duToit N E, Wardle B L, Kim S G 2005 Design considerations for MEMS-scale piezoelectric mechanical vibration energy harvesters *Integ. Ferroelectrics* **71** 121-160
- [7] Horowitz S B, Sheplak M, Cattafesta L N, Nishida T 2006 A MEMS acoustic energy harvester *J. Micromech. Microeng.* **16** S174-S181
- [8] Okamoto H, Onuki T, Kuwano H 2008 Improving an electrets transducer by fully utilizing the implanted charge *Appl. Phys. Lett.* **93** 122901
- [9] Kuwano H, 1993 Research and Development of Sensing Systems within the Framework of Telecommunications – The Paradigm of the Sensor Communication Society *NTT R&D* **42** 913-922
- [10] Kawai H, Kuwano J 1994 Lithium Ion Conductivity of A-Site Deficient Perovskite Solid Solution  $\text{La}_{0.67-x}\text{Li}_{3x}\text{TiO}_3$  *J. Electrochem. Soc.* **141** L78-L79
- [11] Inaguma Y, Liqun C, Itoh M, Nakamura T 1993 High Ionic Conductivity in Lithium Lanthanum Titanate *Solid State Commun.* **86** 689-693
- [12] Hayashi A, Hama S, Minami T, Tatsumisago M 2003 Formation of superionic crystals from mechanically milled  $\text{Li}_2\text{S-P}_2\text{S}_5$  glasses *Electrochem. Commun.* **5** 111-114
- [13] Kanno R, Maruyama M 2001 Lithium Ionic Conductor Thio-LISICON: The  $\text{Li}_2\text{S-GeS}_2\text{-P}_2\text{S}_5$  System **148** A742-A746
- [14] Lapp T, Skaarup S, Hooper A 1983 Ionic Conductivity of Pure and Doped  $\text{Li}_3\text{N}$  *Solid State Ionics* **11** 97-103
- [15] Lubben D, Modine F A 1996 Enhanced ionic conduction mechanisms at  $\text{Li}/\text{Al}_2\text{O}_3$  interfaces *J. Appl. Phys.* **80** 5150-5157
- [16] Schneider A A, Harney D E, Harney M J 1980 The Lithium-Iodine Cell for Medical and Commercial Applications *J. Power Sources* **5** 15-23
- [17] Miwa K, Ohba N, Towata S, Nakamori Y, Orimo S 2004 First-principles study on lithium borohydride  $\text{LiBH}_4$  *Phys. Rev. B* **69** 245120
- [18] Yoshino M, Komiya K, Takahashi Y, Shinzato Y, Yukawa H, Morinaga M 2005 Nature of the chemical bond in complex hydrides,  $\text{NaAlH}_4$ ,  $\text{LiAlH}_4$ ,  $\text{LiBH}_4$  and  $\text{LiNH}_2$  *J. Alloys Compd.* **404-406** 185-190
- [19] van Setten M J, Popa V A, de Wijs G A, Brocks G 2007 Electronic structure and optical properties of lightweight metal hydrides *Phys. Rev. B* **75** 035204
- [20] Soulié J Ph, Renaudin G, Černý R, Yvon K 2002 Lithium boro-hydride  $\text{LiBH}_4$  I. Crystal structure *J. Alloys Compd.* **346** 200-205
- [21] Brinks H W, Hauback B C 2003 The structure of  $\text{Li}_3\text{AlD}_6$  *J. Alloys Compd.* **354** 143-147
- [22] Hauback B C, Brinks H W, Fjellvåg H 2002 Accurate structure of  $\text{LiAlD}_4$  studied by combined powder neutron and X-ray diffraction *J. Alloys Compd.* **346** 184-189
- [23] CRC Handbook of Chemistry and Physics, 88th ed., edited by D. R. Lide (CRC press, Boca Raton, 2007), pp. 12–27.
- [24] Aono H, Sugimoto E, Sadaoka Y, Imanaka N, Adachi G 1993 The Electrical Properties of Ceramic Electrolytes for  $\text{LiM}_x\text{Ti}_{2-x}(\text{PO}_4)_3\text{yLi}_2\text{O}$ ,  $\text{M} = \text{Ge, Sn, Hf, and Zr}$  Systems *J. Electrochem. Soc.* **140** 1827-1833
- [25] Tomita Y, Fujii A, Ohki H, Yamada K, Okuda T 1998 New Lithium Ion Conductor  $\text{Li}_3\text{InBr}_6$  Studied by  $^7\text{Li}$  NMR *Chem. Lett.* **27** 223-224
- [26] Takada K, Aotani N, Iwamoto K, Kondo S 1996 Solid state lithium battery with oxysulfide glass *Solid State Ionics* **86-88** 877- 882
- [27] Kanno R, Hata T, Kawamoto Y, Irie M 2000 Synthesis of a new lithium ionic conductor, thio-LISICON–lithium germanium sulfide system *Solid State Ionics* **130** 97-104
- [28] Filinchuk Y, Chernyshov D, Černý R 2008 Lightest Borohydride Probed by Synchrotron X-ray Diffraction: Experiment Calls for a New Theoretical Revision *J. Phys. Chem. C* **112** 10579-10584
- [29] Fischer D, Müller A, Jansen M 2004 Existiert eine Wurtzit-Modifikation von Lithiumbromid? Untersuchungen im System  $\text{LiBr/LiI}$  *Z. Anorg. Allg. Chem.* **630** 2697-2700
- [30] Sangster J, Pelton A D 1987 Phase Diagrams and Thermodynamic Properties of the 70 Binary Alkali Halide Systems Having Common Ions *J. Phys. Chem. Ref. Data* **16** 509-561
- [31] Maekawa H, Matsuo M, Takamura H, Ando M, Noda Y, Karahashi T, Orimo S 2009 Halide-Stabilized  $\text{LiBH}_4$ , a Room-Temperature Lithium Fast-Ion Conductor *J. Am. Chem. Soc.* **131** 894-895
- [32] Maekawa H, Iwatani T, Shen H, Yamamura T, Kawamura J 2008 Enhanced lithium ion conduction and the size effect on interfacial phase in  $\text{Li}_2\text{ZnI}_4$ -mesoporous alumina composite electrolyte *Solid State Ionics* **178** 1637-1641